The Nature and Role of 8-Deltacyclyl and 7-Isodeltacyclyl Cations in Solvolytic Reactions of Parent Brosylates

Peter K. Freeman* and Jelena E. Dacres

Department of Chemistry, Oregon State University, Corvallis, Oregon 97331

peter.freeman@orst.edu

Received September 4, 2001

Solvolysis of exo-8-deltacyclyl brosylate proceeds directly through a C_2 delocalized cation to exo-8-deltacyclyl acetate. The solvolysis of the endo epimer presents a more complex picture, reacting via a classical deltacyclyl cation, the nonclassical C_2 delocalized cation, and the isodeltacyclyl cation. The solvolysis of exo-7-isodeltacyclyl brosylate generates the 7-isodeltacyclyl ion and subsequently the C_2 delocalized deltacyclyl cation forming 8-deltacyclyl acetate and exo-7-isodeltacyclyl acetate. The cationic intermediates in these three related reaction manifolds are characterized using density functional methods at the B3LYP/6-311+G(3df,2p)//B3LYP/6-31G(d) and BPW91/6-311+G(3df, 2p)//BPW91/6-31G(d) levels.

Introduction

Studies of the 2-norbornyl carbocation (**1**) which were reported by Winstein and Trifan in 1949 have stimulated a half-century of interest in this species.[1] The major focus has been on the participation of the C1−C6 bond in the intermediate and in solvolytic transition states leading to this intermediate.[2] A related system, the deltacyclane system (tetracyclo[4.3.0.0.^{2,4}0^{3,7}]nonane, **2** (X = H) or **2**-H), attracted our attention since it contains a fusion of nortricyclane and norbornane skeletons with the resulting feature that generation of positive charge at C8 could involve participation of the C3−C7 or C2−C3 or C3−C4 bond, or a combination of these, in the resulting intermediate.[3]

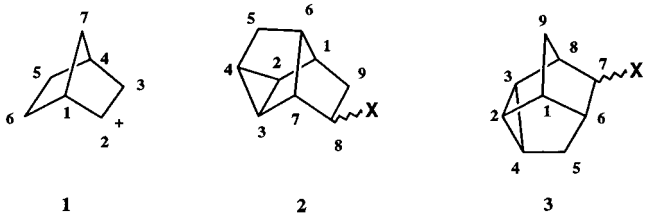

1 **2** **3**

Skeletal rearrangements in the solvolysis of 8-substituted deltacyclanes to give primarily rearranged deltacyclane substrates or isodeltacyclane (tetracyclo-[4.3.0.0.^{2,4}0^{3,8}]nonane) substrates, **3**, were anticipated. Deceptively simple product mixtures were observed. Acetolysis of *exo*- and *endo*-**2**-Cl, deamination of *exo*- and *endo*-**2**-NH_2, and acetolysis of *exo*- and *endo*-**2**-OBs gave a single product, *exo*-**2**-OAc; no endo-substituted products were found. Interestingly, the solvolysis rate of *exo*-**2**-OBs was enhanced by 57-fold relative to the rate of solvolysis of *endo*-**2**-OBs. In addition, the solvolyses of optically active *exo*- and *endo*-**2**-OBs were analyzed for loss of optical activity, which revealed that *endo*-**2**-OBs lost 57% of its optical activity, while *exo*-**2**-OBs retained 99% of its optical activity. To reveal any skeletal rearrangements, *exo*- and *endo*-**2**-OBs were independently labeled with deuterium at C8 and C9 (labeled a and b, respectively, in Scheme 1) and employed in separate experiments. When labeled at C8, products from acetolysis of *endo*-**2**-OBs exhibited a distribution of deuterium over positions 4 and 8; while *endo*-**2**-OBs deuterium labeled at C9 gave scrambling of deuterium over C5 and C9. Both retained 55−60% of the deuterium marker at the original labeled position. Solvolysis of 8- and 9-deuterated *exo*-**2**-

(1) Winstein, S.; Trifan, D. S. *J. Am. Chem. Soc.* **1949**, *71*, 2953; 1952, *74*, 1147, 1154. (b) Lowry, T. H.; Richardson, K. S. *Mechanism and Theory in Organic Chemistry*, 3rd ed.; Harper and Row Publishers: New York, 1987; Chapter 5. (c) Brown, H. C. *The Nonclassical Ion Problem*; Plenum: New York, 1977. (c) Haywood-Farmer, J. *J. Chem. Rev.* **1974**, *74*, 315. (d) Szabo, K. J.; Kraka, E.; Cremer, D. *J. Org. Chem.* **1996**, *61*, 2783. (e) Bethell, D.; Gold, V. *Carbonium Ions, An Introduction*; Academic Press: London, 1967. (f) Prakash, G. K. S. Stable Carbocation Chemistry: Schleyer, P. v. R., Ed.; Wiley: New York, 1996.

(2) Schreiner, P. R.; Schleyer, P. v. R.; Schaefer, H. F., III *J. Org. Chem.* **1997**, *62*, 4216, and refs cited therein.

(3) (a) Freeman, P. K.; Balls, D. M.; Blazevich, J. N. *J. Am. Chem. Soc.* **1970**, *92*, 2051. (b) Freeman, P. K.; Blazevich, J. N. *Chem. Commun.* **1969**, 1357. (c) Freeman, P. K.; Stevenson, B. K. *J. Am. Chem.* Soc. **1973**, *95*, 2890. (d) Freeman, P. K.; Stevenson, B. K.; Balls, D. B.; Jones, D. H. *J. Org. Chem.* **1974**, *39*, 546.

(4) (a) Schleyer, P. v. R.; Watts, W. E.; Fort, R. C., Jr.; Comisarow, M. B.; Olah, G. A. *J. Chem. Am. Soc.* **1964**, *86*, 5679. (b) Saunders: M.; Schleyer, P. v. R.; Olah, G. A. *J. Chem Am. Soc.* **1964**, *86*, 5680.

(5) (a) Hehre, W. J.; Radom, L.; Pople, J. A.; Schleyer, P. v. R. *Ab Initio Molecular Orbital Theory*; John Wiley and Sons: New York, 1986. (b) Jensen, F. *Introduction to Computational Chemistry*; John Wiley and Sons: New York, 1999.

(6) Gaussian 98, Revision A.6, M. J. Frisch, G. W. Trucks, H. B. Schlegel, G. E. Scuseria, M. A. Robb, J. R. Cheeseman, V. G. Zakrzewski, J. A. Montgomery, Jr., R. E. Stratmann, J. C. Burant, S. Dapprich, J. M. Millam, A. D. Daniels, K. N. Kudin, M. C. Strain, O. Farkas, J. Tomasi, V. Barone, M. Cossi, R. Cammi, B. Mennucci, C. Pomelli, C. Adamo, S. Clifford, J. Ochterski, G. A. Petersson, P. Y. Ayala, Q. Cui, K. Morokuma, D. K. Malick, A. D. Rabuck, K. Raghavachari, J. B. Foresman, J. Cioslowski, J. V. Ortiz, B. B. Stefanov, G. Liu, A. Liashenko, P. Piskorz, I. Komaromi, R. Gomperts, R. L. Martin, D. J. Fox, T. Keith, M. A. Al-Laham, C. Y. Peng, A. Nanayakkara, C. Gonzalez, M. Challacombe, P. M. W. Gill, B. Johnson, W. Chen, M. W. Wong, J. L. Andres, C. Gonzalez, M. Head-Gordon, E. S. Replogle, and J. A. Pople, Gaussian, Inc., Pittsburgh, PA, 1998.

(7) (a) Lee, C.; Yang, W.; Parr, R. G. *Phys. Rev. B* **1988**, *37*, 785. (b) Becke, A. D. *Phys. Rev. A* **1988**, *38*, 3098. (c) Becke, A. D. J. *Chem. Phys.* **1993**, *98*, 5648.

(8) Perdew, J. P. *Phys. Rev. B* **1986**, *33*, 8822.

10.1021/jo010897y CCC: $22.00
Published on Web 05/09/2002

Scheme 1

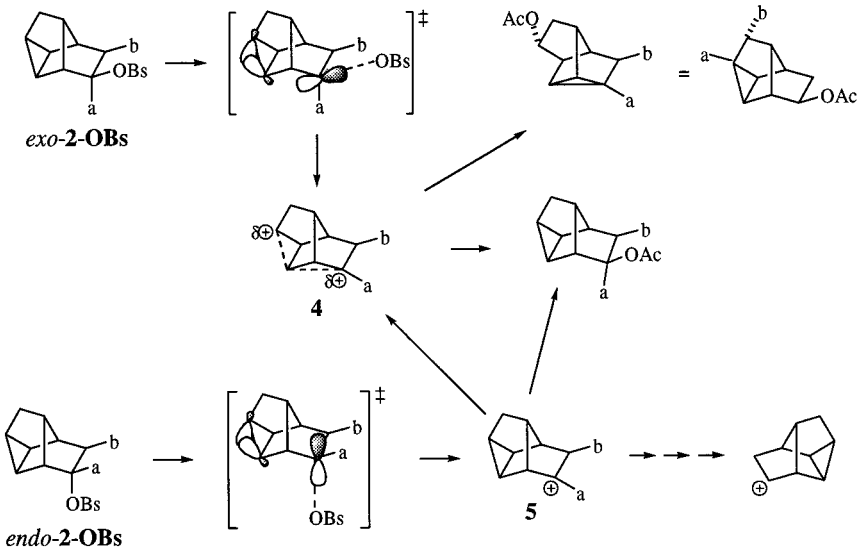

OBs gave the same positional scrambling but the distribution was 50:50 in both cases.

To accommodate these results it was proposed that direct formation of a symmetrical (C_2) delocalized intermediate, **4**, would provide the best mechanistic rationale for the solvolysis of *exo*-**2**-OBs. This proposed delocalized cation, formed through backside anchimeric assistance of the C3−C4 bond, would give the same enantiomer if attacked at either partially charged carbon and, therefore, retain its optical activity during the solvolysis reaction. In addition, a symmetric intermediate would be expected to display a 50:50 scrambling pattern if attacked at the symmetrically equivalent partially charged carbons, as was observed. Finally, a single delocalized intermediate might well be of lower energy than either of the related two rapidly equilibrating classical intermediates in an alternative rationale and would best explain the enhanced rate of solvolysis. The generation of intermediate **4** was supported by the proton NMR of solutions of *exo* and *endo*-**2**-OH in a fluorosulfonic acid−sulfur dioxide solvent.[3a,4]

In the contrasting *endo* case, because the solvolysis of *endo*-**2**-OBs displays a 57% loss of optical activity, the solvolysis cannot be proceeding through an analogous reaction pathway to that of *exo*-**2**-OBs. Therefore, it was suggested that upon solvolysis *endo*-**2**-OBs, in which the forming orbital at the 8 position is poorly lined-up for participation of the C3−C4 bond, must first form localized cation **5**. This localized intermediate could go directly to products, rearrange to form nonclassical cation **4**, or undergo isomerization to form its enantiomer. Clearly, all of localized cation **5** cannot rearrange to form cation **4**. In accordance with loss of optical activity, a maximum of 43% of **5** rearranges to form **4**, leaving 57% of cation **5** to racemize. Racemization via a 1,2-hydride shift would seem to be the simplest explanation. However, a hydride shift from C9 to C8 does not agree with the positional deuterium scrambling. Therefore, we postulated that the racemization of classical cation **5** might comprise a series of alkyl shifts, possibly those in Scheme 2. This scheme includes a series of isodeltacyclyl cations in order to accomplish the required bond shifts. To examine the feasibility of isodeltacyclyl cations as intermediates, deuterated and nondeuterated isodeltacyclanes **3** were prepared.

Scheme 2

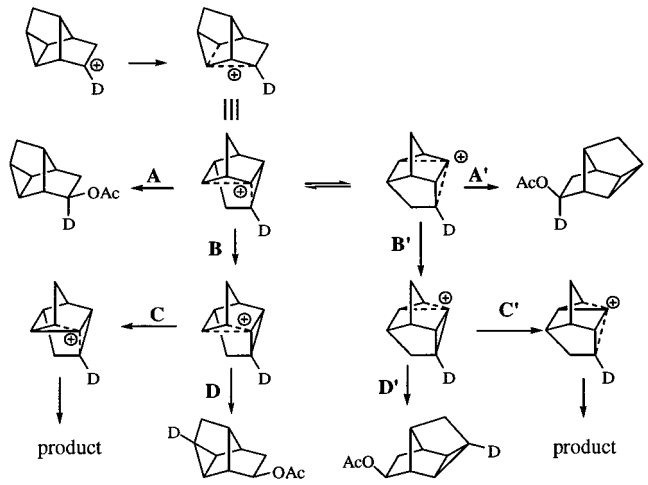

Acetolysis of *exo*-**3**-OBs and *exo*-**3b**-OBs (di-deuterated at C5) gave products *exo*-**2**-OAc and *exo*-**3**-OAc in a 96.7:3.3 ratio, Scheme 3. There was no deuterium scrambling in formed *exo*-**3**-OAc with the entire deuterium label retained at C5. However, in product *exo*-**2**-OAc the deuterium labeled was scrambled between the C9 and C5 in a 1:1.8 ratio. Cations **6**−**9**, Scheme 3, were considered as structures for possible intermediates. Considering the greater deuterium labeling at the C5 position in *exo*-**2**-OAc, it seemed reasonable to propose that the formation of isodeltacyclyl cation **6** with leakage to deltacyclyl cation **4** best explained the experimental results. The existence of cation **9** could not be ruled out since the deuterium label at C5 would not be informative in the case of a Wagner−Meerwein shift of C5 between C6 and C7.

The impetus for additional study lies in the prospect that questions of structure and mechanistic pathway might be answered nicely with ab initio or density functional calculations.

Computational Methods

Calculations on the 8-deltacyclyl and 7-isodeltacyclyl cations and related hydrocarbons employed computational methods that included electron correlation.[5] The hybrid density func-

Scheme 3

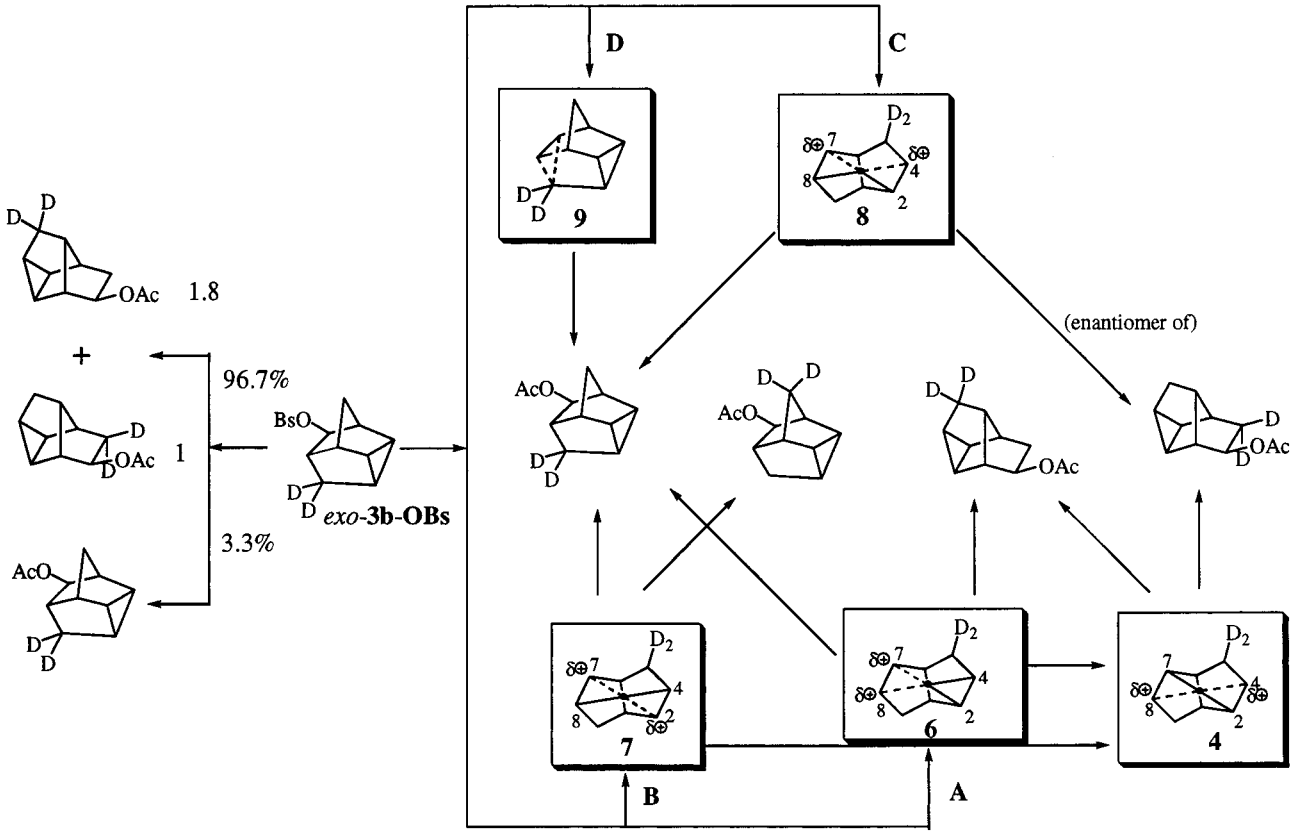

tional and pure density functional techniques pressed into service in this study were the B3LYP and BPW91 methods as implemented in the Gaussian 98 program.[6] All structures were originally minimized using the B3LYP method, where possible.[7] Final optimizations were conducted with the BPW91 density functional method[7b,8] and 6-31g(d) basis set.[9] Final energies were calculated at the BPW91/6-311+G(3df,2p)//BPW91/6-31G(d) or B3LYP/6-311+G(3df,2p)//B3LYP/6-31G(d) level.

Although different starting structures were used in an attempt to isolate the classical 8-deltacyclyl cation, all 8-deltacyclyl cation structures minimized to give a delocalized structure, even at the B3LYP/STO-3G level. Similarly, a geometry optimized structure of 7-isodeltacyclyl cation could only be isolated at the B3LYP/STO-3G and B3LYP/3-21G levels; optimization using the B3LYP method attempted with larger basis sets yielded only the delocalized deltacyclyl cation. The best model geometry for the 7-isodeltacyclyl cation using the B3LYP/6-31G(d) method was obtained from the geometry of the corresponding radical with minor adjustment made by hand to obtain a structure with no imaginary frequencies. Finally, the BPW91/6-31G(d) method produced a minimum structure for the 7-isodeltacyclyl cation. However, the BPW91/6-31G(d) method was unable to locate the classical 8-deltacyclyl cation and produced only delocalized deltacyclyl cation **4**. Therefore, model geometries for the classical 8-deltacyclyl cation were obtained by calculating the minimum energy structure for the corresponding radical using both the B3LYP/6-31G(d) and BPW91/6-31G(d) methods. These structures proved to have no imaginary frequencies when single point calculations were performed. When solvent was included, optimizations using the polarizable continuum model (PCM) of Tomasi et al.[10] and the dielectric constant for the original solvent, acetic acid, at the HF/6-31+G* and BPW91/6-31G* levels, an ion more classical than symmetrical **4,** labeled as **5′**, was isolated.

Results and Discussion

A gratifying result from the calculations is the confirmation of the nonclassical nature of the deltacyclyl cation, **4**, originally proposed, Figure 1. Proton NMR calculations of **4** were completed at the B3LYP/6-311+G(2d,p)//B3LYP/6-31G(d) and RHF/6-311+G(2d,p)//B3LYP/6-31G(d) level.[11] The results, as shown in Table 1, are in rough agreement with experiment[12] with a standard deviation of 1.11 δ and 1.25 δ for the B3LYP and RHF calculations, respectively. Both methods show difficulty in accurately calculating the NMR shift for the proton on pentavalent carbon 3, but do indicate the C_2 symmetry. The greatest downfield shift for the equivalent protons at C4 and C8 is in agreement with the structural representation of **4**. The second greatest downfield shift belongs to the equivalent protons at C2 and C7. Consistent with this,

(9) Petersson, G. A: Bennett, A.; Tensfeldt, T. G.; Al-Laham, M. A.; Shirley, W. A.; Mantzaris, J. *J. Chem. Phys.* **1988**, *89*, 2193−2218. Petersson, G. A.; Al-Laham, M. A. *J. Chem. Phys.* **1991**, *94*, 6081−6090.

(10) Miertus, S.; Scrocco, E.; Tomasi, *J. Chem. Phys.* **1981**, *55*, 117−129. Miertus, S.; Tomasi, J. *Chem. Phys.* **1982**, *65*, 239−245. Cossi, M.; Barone, V.; Cammi, R.; Tomasi, J. *Chem. Phys. Lett.* **1996**, *255*, 327−335. Barone, V.; Cossi, M.; Tomasi, J. *J. Comput. Chem.* **1998**, *19*, 404−417.

(11) (a) Wolinski, K.; Hilton, J. F.; Pulay, P. *J. Am. Chem. Soc.* **1990**, *112*, 8251−8206. (b) Foresman, J. B.; Frisch, A. *Exploring Chemistry with Electronic Structure Methods*, 2ns ed.; Gaussian, Inc.: Pittsburgh, 1996; Chapter 2. (c) Cheeseman, J. R.; Trucks, G. W.; Keith, T. A.; Frisch, M. J. *J. Chem. Phys.* **1996**, *104*, 5497.

(12) Since the experimental HNMR values were determined using a Varian Associates A-60 or HA-100 NMR spectrometer without the aid of two-dimensional techniques such as COSY or HETCOR, the assignments for the delta shift values for **4** were changed from the original ones to achieve better agreement with the calculated values (ref 3a).

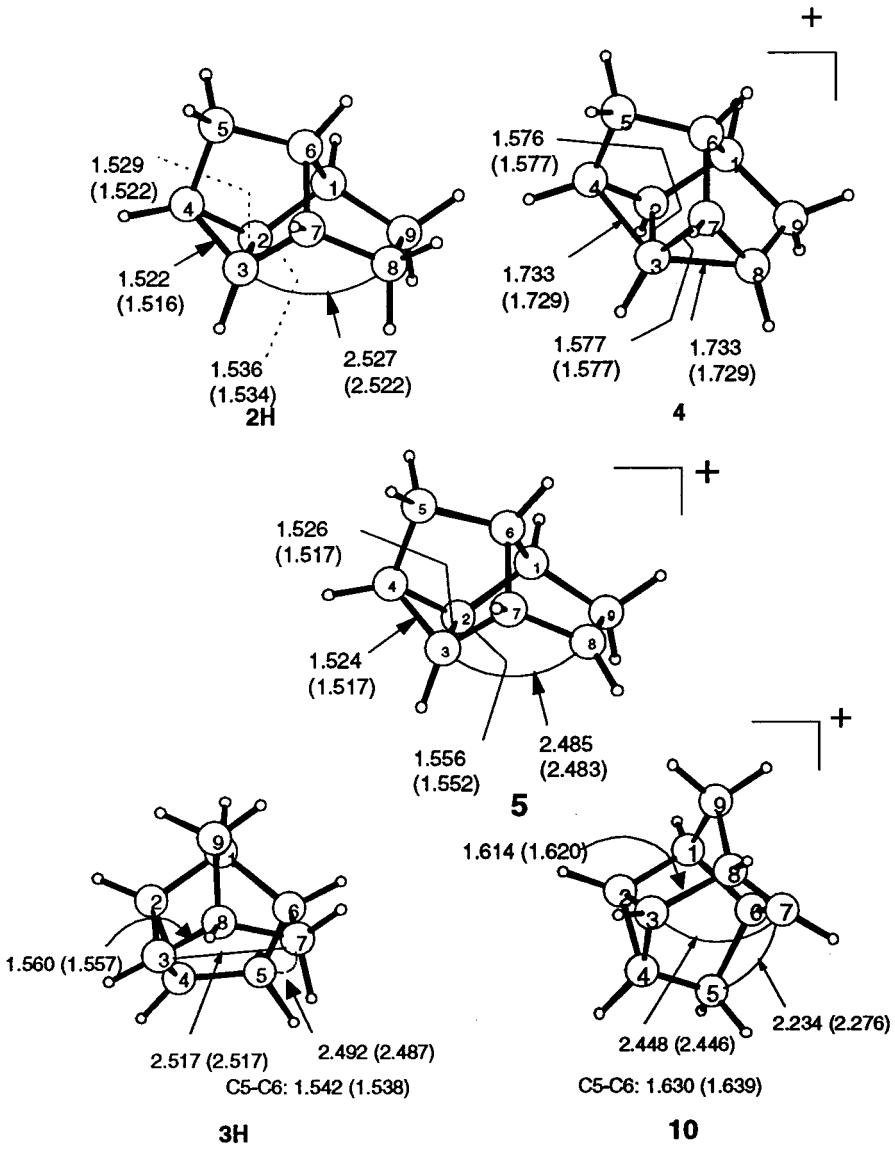

Figure 1. Geometry optimized structures for **2H**, **3H**, **4**, **5**, and **10** at the BPW91/6-31G(d) level (in parentheses are the B3LYP/6-31G(d) geometries for **2H**, **3H**, **4**, and **5** and the B3LYP/3-21G geometry for **10**).

Table 1. Calculated and Experimental ^{1}H NMR[a] Shifts for Nonclassical Deltacyclyl Cation 4

hydrogen on carbon	B3LYP/6-311+G(2d,p)// B3LYP/6-31G(d) (δ)	RHF/6-311+G(2d,p)// B3LYP/6-31G(d) (δ)	exptl[b] (δ)
1	2.71	2.47	1.77
2	4.48	4.34	2.92
3	−0.43	−1.04	2.17
4	5.77	5.54	5.17
5-*endo*	3.30	3.05	2.50
5-*exo*	2.69	2.47	1.77
6	2.71	2.48	1.77
7	4.48	4.34	2.92
8	5.77	5.55	5.17
9-*endo*	3.30	3.05	2.50
9-*exo*	2.69	2.48	1.77

[a] GIAO method, ref 11. [b] Reference 3a.

the structure of **4** clearly shows long bonds for C3−C8 and C3−C4 as well as some lengthening at C3−C7 and C3−C2. Both the B3LYP/6-31G(d) and the BPW91/6-31G(d) structures reveal carbon−carbon distances for C3−C8 and C3−C4 that are 1.73 Å, which compares with the long C−C bonds slightly greater than 1.70 Å described by Kammermeier et al.,[13] and give the intermediate essentially C_2 symmetry. Interestingly, the calculated geometry for deltacyclyl cation **4** shows a small amount of norbornonium ion delocalization with the C7−C3 and C3−C2 bonds at 1.577 and 1.576 Å. The equivalent bond (the C6−C1 bond) in 2-norbornyl cation is 1.863 Å at the BPW91/6-31G(d) and 1.891 Å at the B3LYP/6-31G(d) level; these results compare favorably with the MP2/6-31G(d) C1−C6 bond distance of 1.829 Å reported by Schleyer.[14] All methods give the 2-norbornyl cation a C_S symmetry, Figure 2.

Attempts to isolate the classical deltacyclyl cation and the isodeltacyclyl cation computationally confronted the problem that all the cations calculated tended to optimize to the nonclassical deltacyclyl cation. Many manipulations of Gaussian calculations, including restricted optimizations, reduced step-size, and reading in force constants, were attempted in the hope of isolating the

(13) Kammermeier, S.; Jones, P. G.; Herges, R. *Angew. Chem., Int. Ed. Engl.* **1997**, *36*, 1757−1759.

(14) (a) Sieber, S.; Schleyer, P. v. R.; Vancik, H.; Mesic, M.; Sunko, D. E. *Angew. Chem., Int. Ed. Engl.* **1993**, *32*, 1604. (b) Schleyer, P. v. R.; Sieber, S. *Angew. Chem., Int. Ed. Engl.* **1993**, *32*, 1606.

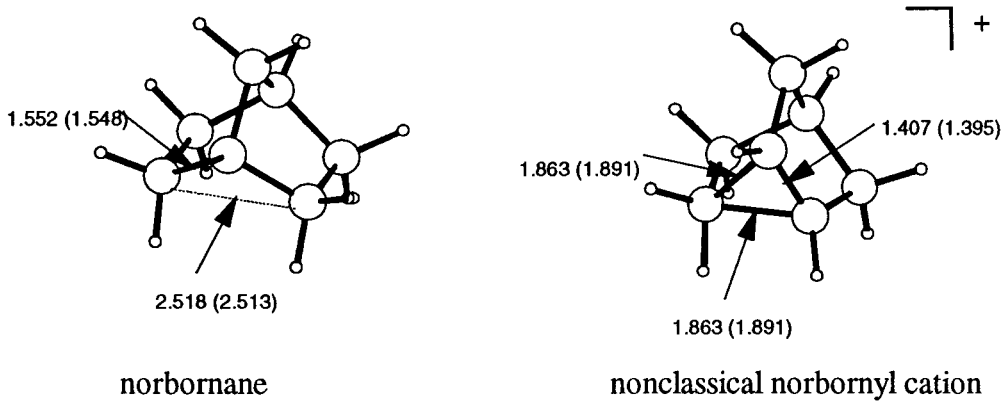

Figure 2. Geometry optimized structures for norbornane and the 2-norbornyl cation at the BPW91/6-31G(d) level (B3LYP/6-31G(d) geometries in parentheses).

Table 2. Energies and Isodesmic Reaction Energies[a] for Cations 4, 5, and 10 Using the BPW91/6-311+G(3df,2p)//BPW91/6-31g(d)[b] Method (BPW91/6-31g(d)//BPW91/6-31g(d) Method in Parentheses)

isodesmic reactions	cation$_{(i)}$ E + ZPE (au)	hydrocarbon$_{(i)}$ E + ZPE (au)	cation$_{(f)}$ E + ZPE (au)	hydrocarbon$_{(f)}$ E + ZPE (au)	ΔE (kcal/mol)
deltacyclyl cation **4**	−349.14197	−273.83065	−272.94583	−350.01880	5.0
	(−349.04366)	(−273.74556)	(−272.86527)	(−349.91342)	(6.6)
classical deltacyclyl cation **5**	−349.12079	−273.83065	−272.94583	−350.01880	−8.3
	(−349.02210)	(−273.74556)	(−272.86527)	(−349.91342)	(−6.9)
isodeltacyclyl cation **10**	−349.11343	−273.83065	−272.94583	−350.00592	−4.8
	(−349.01394)	(−273.74556)	(−272.86527)	(−349.90080)	(−4.1)

[a] $\Delta E = ((E_H + ZPE)_{(f)} + (E_C + ZPE)_{(f)} - (E_H + ZPE)_{(i)} - (E_C + ZPE)_{(i)}) \times 627.5095$. [b] ΔE for BPW91/6-311+g(3df,2p)//BPW91/6-31g(d) include the energies at the BPW91/6-311+g(3df,2p)//BPW91/6-31g(d) level plus zero point energies at the BPW91/6-31g(d)//BPW91/6-31g(d) level.

Table 3. Energies and Isodesmic Reaction Energies[a] for Cation 4, and Models[b] for Cations 5 and 10 Using the B3LYP/6-311+G(3df,2p)//B3LYP/6-31g(d)[c] Method (B3LYP/6-31g(d)//B3LYP/6-31g(d) in Parentheses)

isodesmic reactions	cation$_{(i)}$ E + ZPE (au)	hydrocarbon$_{(I)}$ E + ZPE (au)	cation$_{(f)}$ E + ZPE (au)	hydrocarbon$_{(f)}$ E + ZPE (au)	ΔE (kcal/mol)
deltacyclyl cation **4**	−349.17891	−273.88197	−272.98460	−350.06611	6.4
	(−349.07733)	(−273.79050)	(−272.90082)	(−349.95760)	(5.9)
classical deltacyclyl cation **5**	−349.15795	−273.88197	−272.98460	−350.06611	−6.8
	(−349.05601)	(−273.79050)	(−272.90082)	(−349.95760)	(−7.5)
isodeltacyclyl cation **10**	−349.13386	−273.88197	−272.98460	−350.05290	−13.6
	(−349.03380)	(−273.79050)	(−272.90082)	(−349.94476)	(−13.4)

[a] $\Delta E = ((E_H + ZPE)_{(f)} + (E_C + ZPE)_{(f)} - (E_H + ZPE)_{(i)} - (E_C + ZPE)_{(i)}) \times 627.5095$. [b] Energies for cations **5**and **10** are vertical ionization energies from the corresponding radicals. [c] ΔE for B3LYP/6-311+g(3df,2p)//B3LYP/6-31g(d) include the energies at the B3LYP/6-311+g(3df,2p)//B3LYP/6-31g(d) level plus zero point energies at the B3LYP/6-31g(d)//B3LYP/6-31g(d) level.

higher energy cations at the B3LYP/6-31G(d) level, but to no avail. However, a geometry optimized structure for the isodeltacyclyl cation was found using the BPW91/6-31G(d) method (Figure 1). Despite the success of finding the isodeltacyclyl cation, calculations at the same level on the classical deltacyclyl cation optimized to give the nonclassical deltacyclyl cation. Therefore, in the case of classical deltacyclyl cation, a model calculation was analyzed using vertical ionization from the optimized structure of the corresponding radical (Figure 1).[2]

The BPW91/6-31g(d) geometry optimized structures reveal that the C3−C8 and C5−C6 are 0.054 and 0.088 Å longer in isodeltacyclyl cation than in isodeltacyclane. The lengthening of these bonds and the contraction of the C3−C7 distance by 0.069 Å provides a structural anticipation of a Wagner−Meerwein shift of either C3 or C5. The minimum energy structure for isodeltacyclyl cation, **10**, does not correspond to any single intermediate proposed previously[3d] but rather to a combination of possible intermediates **6** and **9**. The model geometry for classical deltacyclyl cation **5** is quite similar to that for deltacyclane, since it is derived from the radical geometry.

Isodesmic equations, such as that illustrated in eq 1,

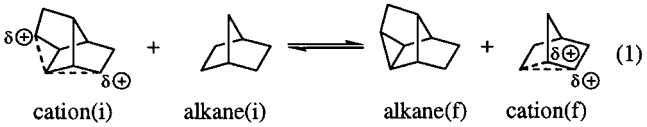

(1)

were employed to calculate the stabilization energies (ΔE at the BPW91/6-311+G(3df,2p)//BPW91/6-31G(d) level, Table 2) of cations **4**, **5**, and **10** relative to the known delocalized 2-norbornyl cation (stabilization energies using the B3LYP/6-311+G(3df,2p)//B3LYP/6-31G(d) method are listed in Table 3). It is readily apparent that nonclassical deltacyclyl cation **4**, being even more stable than 2-norbornyl cation (ΔE = 5.0 kcal/mol), is the most stabilized species in this study. Isodeltacyclyl cation **10** is a distant second (ΔE = −4.8 kcal/mol), followed by classical deltacyclyl cation **5** (ΔE = −8.3 kcal/mol). Both **10** and **5** are less stabilized than 2-norbornyl cation which is reflected in the isodesmic reaction favoring the right

Scheme 4

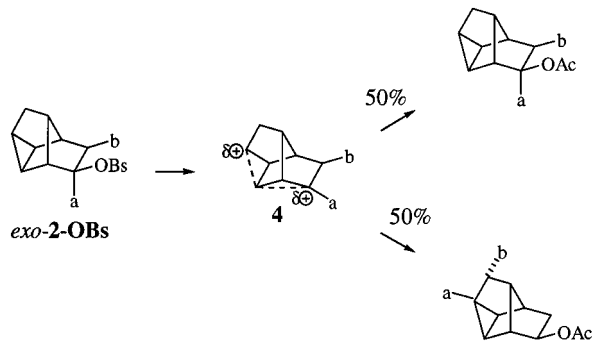

Scheme 5

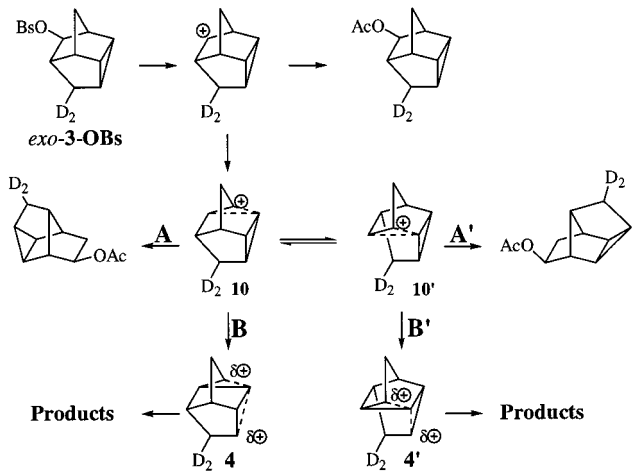

side of the equation. Notably, nonclassical cation **4** is 13.3 kcal/mol more stable than classical cation **5**, which is a stabilizing energy difference (BPW91/6-311+G(3df,2p)//BPW91/6-31G(d) that is remarkably similar to the 13−14 kcal/mol energy difference (B3LYP//6-311+G(d)//B3LYP/6-31G(d) calculated by Schleyer and co-workers[2] for classical and nonclassical 2-norbornyl cations. These energies of stabilization when combined with the experimental data create an intriguing image of the solvolyses of *exo*- and *endo*-**2-OBs** and *exo*-**3-OBs**.

Unlike the solvolyses of *exo*- and *endo*-2-norbornyl brosylates, where the products derived are completely racemized, the solvolyses of *exo*- and *endo*-**2**-OBs give different racemization ratios and different ratios of deuterium scrambling. Therefore, the idiosyncrasies in solvolysis rates for *exo*- and *endo*-**2**-OBs cannot be from transition structures that lead to the same intermediate, as is proposed by Schleyer and co-workers for the 2-substituted norbornyl systems.[2] Instead, the solvolyses of *exo*- and *endo*-**2**-OBs must initially produce two different cations. Considering that the solvolysis of *exo*-**2**-OBs is 57 times faster than the solvolysis of *endo*-**2**-OBs, the rates of C-5 substituted *exo*-**2**-OBs are more sensitive to polar effects than similarly substituted *endo*-**2**-OBs ($\rho_{exo} = -2.68$, $\rho_{endo} = -1.63$),[3c] the secondary β-deuterium isotope effect for *exo*-9-deuterio-*endo*-**2**-OBs is greater than that for *exo*-9-deuterio-*exo*-**2**-OBs,[3b] and the C3−C4 bond of **2** is in an excellent position to provide backside anchimeric assistance to *exo*-**2**-OBs, *exo*-**2**-OBs must proceed directly to cation **4**, Scheme 4, which then gives a 50−50 deuterium scrambling ratio.

Consideration of the solvolysis of *exo*-**3**-OBs reveals that nonclassical deltacyclyl cation **4** also lies along this

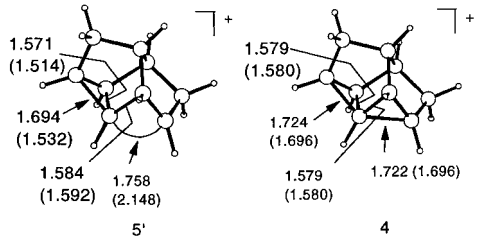

Figure 3. Geometry optimized structures for **5′** and **4** in acetic acid using the SCRF(PCM) method at the BPW91/6-31G(d) and (in parentheses) HF/6-31+G(d) levels.

reaction pathway. First, the products from the solvolysis of *exo*-**3**-OBs display similar deuterium scrambling as that seen in the solvolysis of *exo*-**2**-OBs. Second, the calculated structure for isodeltacyclyl cation **10** reveals a long bond (1.614 Å) between carbons 3 and 8. A Wagner−Meerwein shift of C3 from C8 to C7 would give a cation with a deltacyclyl structure. If this 1,2-carbon shift were accompanied by anchimeric stabilization from the C3−C4 bond, then nonclassical deltacyclyl cation **4** would be formed. A classical isodeltacyclyl cation formed directly upon solvation of *exo*-**3**-OBs cannot be ruled out since 3.3% of exo-**3**-OAc was formed. If this classical ion is formed, then the majority of it proceeds to **10**, Scheme 5. Since cation **4** gives a 50:50 deuterium scrambling ratio, and the products from the solvolysis of *exo*-**3**-OBs display a 64.3% retained to 35.7% relocated deuterium label, there must be a competition between direct attack of HOAc/OAc^- on **10** (pathway A, Scheme 5) and rearrangement of **10** to deltacyclyl cation **4** (pathway B, Scheme 5). Analysis of the products reveals that rearrangement of **10** to **4** is favored 2.5 times over direct attack of HOAc/OAc^- on **10**.

Returning to the *endo*- vs *exo*-**2**-OBs problem, *endo*-**2**-OBs most likely forms classical cation **5** (or at least an ion more classical than **4**) first for the reasons given. As suggested by a referee, it may be necessary to include solvent in the calculation in order to demonstrate that there is a cation more classical than **4** which proceeds it in the solvolysis of endo-**2**-OBs. Using the polarizable continuum model of Tomasi and co-workers[10] and the dielectric constant for the original solvent acetic acid, optimizations at HF/6-31+G* and BPW91/6-31G* reveal an ion more classical than **4** (labeled as **5′**) with a definite asymmetry for C-3−C-8 (2.148 and 1.758 at HF 6-31+G* and BPW91/6-31G*) and C-4−C-3 (1.532 and 1.694 at HF/6-31+G* and BPW91/6-31G*) (Figure 3). These structural features can be compared with those of nonclassical **4** in acetic acid at these same levels (Figure 3). It is important to note that calculations starting with a classical 8-deltacyclyl framework at HF/6-31+G* or BPW91/6-31G* without solvent lead to symmetrical nonclassical cation **4**. These calculational results with solvent for cations **5′** and **4** are not as persuasive as one might hope. The geometries are very close, as well as the energies at BPW91/6-31G* (**5′** 2.3 kcal/mol above **4**), and we could not get the frequency calculation on **5′** to converge on maximum displacement. This does provides support, however, for an ion more classical than **4**. Once formed, an ion we suggest is similar to **5** or **5′** has three pathways to follow: go directly to product, form nonclassical cation **4**, or undergo a cyclopropylethyl to cyclopropylethyl shift to form isodeltacyclyl cation **10** (Scheme 6). Product analysis reveals that **5** (**5′**) takes all

Scheme 6

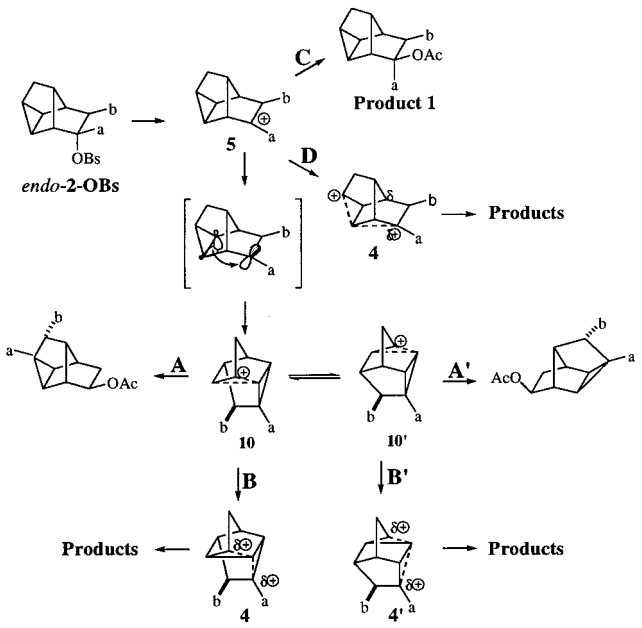

three pathways. Of the paths available, only rearrangement of deltacyclyl cation **5** (**5′**) to isodeltacyclyl cation **10** allows for racemization. One might expect that a norbornyl type 1,2-carbon shift of C3 in deltacyclyl cation **5** (**5′**) from C7 to C8 would be the simplest route from **5** (**5′**) to **10**. However, this Wagner−Meerwein shift and **10** ⇌ **10′** would move a deuterium originally labeled at C8 to C1, which was not observed. Conversely, if C3 were shifted from C2 to C8, then a deuterium originally positioned at C8 would be moved to C4 which was observed. As revealed by the calculated structure for **10**, a Wagner−Meerwein shift of C5 from C6 to C7 is, to a degree, anticipated in the partially delocalized C5−C6 bond of intermediate **10** and would produce the enantiomer of **10**.

According to the loss of optical activity in the solvolysis of *endo*-**2**-OBs, 57% of **5** (**5′**) follows the path through **10**(**10′**), Scheme 6. Using the above observation that **10** will rearrange to form **4** 2.5 times more than **10** will be directly attacked by HOAc/OAc$^-$, the 57% of **5**(**5′**) that rearranges to **10**(**10′**) works out to react 40.7% through pathways B and B′, and 16.3% through pathways A and A′, Scheme 6. The remaining 43% of **5**(**5′**) follows pathway C 36.3% of the time and directly rearranges to form nonclassical cation **4**, pathway D, only 6.7% of the time. The C/D division is 26.3/16.7 if the 55% value for the retention of label at the original position in *endo*-**2**-OBs is used. These concomitant steps account for the loss of optical activity, the greater deuterium label retained at its original position, and the slower rate of solvolysis for *endo*-**2**-OBs.

Conclusions

The best representation of the lowest energy structure for 8-deltacyclyl cation is ion **4**. The nonclassical nature of cation **4** is revealed by a consideration of structural and energetic relationships with related species. The delocalization of charge principally involving the perimeter cyclopropane bond provides C_2 symmetry and bonds (1.73 Å) between carbon 3 and carbons 4 and 8. Using isodesmic reactions and direct comparisons, nonclassical ion **4** is 5.0 kcal/mol more stable than 2-norbornyl, 9.8 kcal/mol more stable than isodeltacyclyl (**10**), and 13.3 kcal/mol more stable than a model for classical deltacyclyl cation. Solvolysis of *exo*-8-deltacyclyl brosylate proceeds directly to intermediate **4**, which generates product, whereas both *endo*-**2**-OBs and *exo*-**3**-OBs first form cations upon acetolysis that are less delocalized than **4**, subsequently creating cation **10** and then **4**, both of which generate product. Although intuition predicts that deltacyclyl cation **5**(**5′**)would readily delocalize to form nonclassical deltacyclyl cation **4**, this turns out to occur less rapidly than conversion to isodeltacyclyl ion **10**. It is clear that the special stability of nonclassical cation **4** allows it to be an intermediate on the reaction pathway for the solvolyses of *exo*- and *endo*-**2**-OBs, and *exo*-**3**-OBs.

Acknowledgment. Support from the Oregon State University Research Council, the MRF fund, and the NIEHS is gratefully acknowledged.

Supporting Information Available: Cartesian coordinates for all optimizations described are available free of charge on the Internet at http://pubs.acs.org.

JO010897Y